ELSEVIER

Journal of Structural Geology 27 (2005) 1155–1167

JOURNAL OF STRUCTURAL GEOLOGY

www.elsevier.com/locate/jsg

Instability of an anisotropic power-law fluid in a basic state of plane flow

Raymond C. Fletcher

Department of Geosciences, Pennsylvania State University, University Park, PA 16803, USA

Received 28 August 2003; received in revised form 19 February 2004; accepted 31 August 2004

Abstract

Initiation of cylindrical structures by buckling or necking in an anisotropic power-law fluid is treated for general plane flow. The principal axis of anisotropy, x', in the stiffest direction in shortening or extension may be viewed as the trace of a foliation or lamination. Plane-flow constitutive relations between components of rate of deformation, D'_{xx} and D'_{xy}, and of deviatoric stress, s'_{xx} and s'_{xy}, for the fluid are $D'_{xx} = B(Y'_2)^{[(n-1)/2]}s'_{xx}$ and $D'_{xy} = a^2B(Y'_2)^{[(n-1)/2]}s'_{xy}$, where $Y'_2 = (s'_{xx})^2 + a^2(s'_{xy})^2$ is an anisotropic invariant, a^2 is the anisotropy parameter, and n is the stress exponent. We determine the rate of amplification of wavelength components in the deflection of the foliation, θ, from a mean orientation parallel to x. Linearly independent, or non-interacting normal modes have a periodic, band-like form $\theta(x, y) \cong \partial\zeta/\partial x = -(\lambda A)\sin[\lambda(x - vy)]$, where ζ is the height of a foliation trace above its mean plane, $v = \tan\beta$, where β is the angle between the normal to mean foliation and the axial surface, positive *clockwise*, and $L = 2\pi/\lambda$ is the foliation-parallel wavelength. Evolution of a component may be followed through a finite bulk deformation provided θ remains $\ll 1$. The growth rate of slope, λA, is independent of L.

Components with axial plane normal to the foliation ($\beta = 0$) are strongly amplified in foliation-parallel shortening. If $n >> 1$, internal necking (boudinage) occurs in foliation-parallel extension for components with axial plane inclined at a large angle to the foliation normal. In combined shortening and shear, the most rapidly growing component has an axial plane that dips steeply in the direction of shear. For $n > 1$, maximum instability occurs for combined foliation-parallel shear and shortening rather than pure shortening. Weak instability is present in foliation-parallel shear.

This anisotropic nonlinear fluid approximates the behavior of an isotropic power-law medium containing preferentially oriented but anastomosing slip surfaces, or that of a rock in which a stiffer component of lenticular form is embedded in a softer matrix.

Keywords: Anisotropic power-law fluid; Plane flow; Foliation; Lamination

1. Introduction

An anisotropic continuum with the bulk behavior of a composite rock that is layered, made up of aligned lenticular elements, or has lattice preferred orientation may be used to model several types of tectonic structures (Bayly, 1964; Cobbold et al., 1971; Cobbold, 1976) whose scale is much greater than the *microscopic* scale of the composite's constituents. For example, Bayly (1964, 1970, 1974) modeled similar folding in an anisotropic viscous fluid. Casey and Huggenberger (1985) used this mathematically one-dimensional analysis to treat finite-amplitude folding for an arbitrary history of bulk deformation. Cobbold et al. (1971) applied a formulation and analysis of Biot (1965a) to show how structures produced in naturally and experimentally deformed materials could be interpreted as modes of internal instability of an anisotropic medium. Latham (1985a,b) incorporated into this analysis the rheological nonlinearity of the constituents of a bilaminate material and the bending resistance of the constituent layers.

The results of Cobbold et al. (1971) and Latham (1985a,b) are based on a formulation and analysis for incremental deformation of an *elastic* or *viscoelastic* material and in a limiting sense, to a *viscous fluid*. It is less clear that Latham's treatment applies to a linear or nonlinear viscous fluid. A condition for such application is that the instability be sufficiently strong to establish

E-mail address: rfletche@geosc.psu.

0191-8141/$ - see front matter © 2004 Elsevier Ltd. All rights reserved.
doi:10.1016/j.jsg.2004.08.002

Table of symbols

A	amplitude
a^2	anisotropy parameter
a	square root of anisotropy parameter
B, B_1, B_2, B^*	constants in power-law relations
d_{xx}, d_{xy}	normalized rate of deformation components
D_{xx}, D_{yy}, D_{xy}	components of rate of deformation tensor referred to solution axes
D'_{xx}, D'_{yy}, D'_{xy}	components of rate of deformation referred to principal axes of anisotropy
$\bar{D}_{xx}$, $\bar{D}_{yy}$, $\bar{D}_{xy}$	components of rate of deformation of the basic-state
$\tilde{D}_{xx}$, $\tilde{D}_{yy}$, $\tilde{D}_{xy}$	perturbing values of components of rate of deformation
f_1, f_2	volume fractions of constituents
h, h_s	functions in the flow law of a plastic solid
$\bar{I}_2$	basic-state rate of deformation invariant
$J_2^{(1)}$, $J_2^{(2)}$, J_2	component and bulk isotropic stress invariants
K	maximum shear stress at yield
L	wavelength
M, M^*, N, N^*	quantities used in perturbation analysis
m	principal viscosity ratio
n, n_1, n_2, n^*	component and bulk stress exponents
q, q_{MECH}, $q_{\max}$	relative growth rate parameters
s_{xx}, s_{xy}	deviatoric stress components referred to solution axes
s'_{xx}, s'_{xy}	deviatoric stress components referred to principal axes of anisotropy
$\bar{s}_{xx}$, $\bar{s}_{yy}$	basic-state deviatoric stress components
$\tilde{s}_{xx}$, $\tilde{s}_{yy}$	perturbing deviatoric stress components
$s_{xx}^{(1)}$, $s_{xx}^{(2)}$	deviatoric stress components in materials 1 and 2
v_x, v_y	velocity components
$\bar{v}_x$, $\bar{v}_y$	basic-state velocity components
x, y	fixed solution axes
x', y'	principal axes of anisotropy
X	dummy function
Y'_2, $\bar{Y}_2$	anisotropic invariant, referred to principal axes of anisotropy and basic state
β	angle between normal to mean foliation and axial plane of band
δ	angle of slip surface in anisotropic plastic solid
Γ	shear strain
η_1, η_2	viscosities of two isotropic fluids
η_{n}, η_{s}	bulk principal normal and shear viscosities
λ	wavenumber
Λ	quantity used in perturbation analysis
ν	$\tan(\beta)$
Π, Π'	functions of invariants or anisotropic invariants of deviatoric stress
ϕ	Airy stress function
σ_{xx}, σ_{yy}, σ_{xy}	stress components
θ	angle of principal axis x' or of 'foliation' from the x-axis, positive anticlockwise
Θ	slope amplitude
ζ	height of foliation above mean plane

structure after small bulk deformation, as in folding of a single layer by interfacial instability (Biot, 1961). The condition is removed in Biot's (1964) exact analysis of folding of a viscous layer, and in the analysis of Sherwin and Chapple (1968). No restriction on strain magnitude is imposed in the analyses of Bayly (1964), Cobbold (1976), and Casey and Huggenberger (1985).

This paper deals with the inception of cylindrical structures in a nonlinear anisotropic fluid in general plane flow. The components in the geometric perturbation are periodic, cylindrical deflections, θ, about the mean in the orientation of a principal axis of anisotropy, or *foliation*. Provided θ remains small, perturbation growth may be followed through large basic-state deformation. Since internal instability in rock may be moderate to weak, regular structure may only emerge after large deformation. The form of the cylindrical perturbation and the basic-state rates of shortening or extension and shear parallel to the foliation are arbitrary. This removes the restriction to orthotropic cases in Cobbold et al. (1971) and Latham (1985a,b). The formulation and analysis applies only to an anisotropic fluid, excluding elastic and viscoelastic effects.

2. Constitutive relations

2.1. Introduction

Deformation of layered, laminated, or foliated rocks at a scale that is large relative to the dimensions of their microscopic structure components is well approximated by treating the rock as a homogeneous anisotropic medium (Bayly, 1964; Biot, 1965a,b; Cobbold, 1976). Bayly (1964) treated an anisotropic linear viscous fluid, the properties of which consist of two principal viscosities, η_{n} in lamination-parallel or lamination-normal shortening or extension, and η_{s} in lamination-parallel or lamination-normal shear. If the laminations are alternating layers of isotropic fluid with viscosities η_1 and η_2 and thickness fractions f_1 and f_2, the bulk principal viscosities are exactly

$$\eta_{\mathrm{n}} = f_1\eta_1 + f_2\eta_2, \quad \eta_{\mathrm{s}} = (f_1/\eta_1 + f_2/\eta_2)^{-1}. \tag{1}$$

To treat a fuller range in behavior in which structures such as internal boudinage (Cobbold et al., 1971; Platt and Vissers, 1980) are possible it is necessary to consider

nonlinear anisotropic materials. The equivalent issue for interfacial instability in discrete layers composed of isotropic materials is addressed by Biot (1961) in the thin-plate approximation, and by Parrish (1973), Fletcher (1974), and Smith (1977, 1979).

If a layered material is composed of two isotropic power-law fluids, exact macroscopic constitutive relations may be derived from the component constitutive relations together with conditions of interfacial coherence and stress averaging. They are

$$D_{xx} = -D_{yy} = B_1\left[J_2^{(1)}\right]^{[(n_1-1)/2]} s_{xx}^{(1)} = B_2\left[J_2^{(2)}\right]^{[(n_2-1)/2]} s_{xx}^{(2)},$$
$$D_{xy} = \left\{f_1 B_1\left[J_2^{(1)}\right]^{[(n_1-1)/2]} + f_2 B_2\left[J_2^{(2)}\right]^{[(n_2-1)/2]}\right\} s_{xy}. \tag{2}$$

where the isotropic invariants are of the form

$$J_2^{(1)} = \left(s_{xx}^{(1)}\right)^2 + \left(s_{xy}\right)^2.$$

The normal components of the deviatoric stress within the constituent layers are $s_{xx}^{(1)}$ and $s_{xx}^{(2)}$ and the bulk layer-parallel value is

$$f_1 s_{xx}^{(1)} + f_2 s_{xx}^{(2)} = s_{xx}. \tag{3}$$

where s_{xx} and s_{xy} are the bulk deviatoric stress components. B_1 and B_2 are constants, and n_1 and n_2 are the stress exponents of the constituents. All deviatoric stress components in plane flow of an incompressible fluid are related to the corresponding stress components according to

$$s_{xx} = 1/2\left(\sigma_{xx} - \sigma_{yy}\right), \quad s_{xy} = \sigma_{xy}. \tag{4}$$

The rate of deformation components are related to the velocity components v_x and v_y through the kinematic relations

$$D_{xx} = \partial v_x/\partial x, \quad D_{yy} = \partial v_y/\partial y,$$
$$D_{xy} = 1/2\left(\partial v_y/\partial x + \partial v_x/\partial y\right). \tag{5}$$

The relations (2) are difficult to use because they incorporate the constituent or microscopic normal components in nonlinear expressions. In the linear case, $n_1 = n_2 = 1$, the microscopic components may be eliminated once and for all to obtain (1). Here, we aim to establish simpler nonlinear relations that only involve macroscopic components of stress and rate of deformation.

2.2. Anisotropic materials formed by introducing parallel slip surfaces in an isotropic material

Cobbold et al. (1971) discuss in qualitative terms a material that consists of a homogeneous isotropic medium containing a closely-spaced set of weak slip surfaces (IMSS fluid). Its bulk constitutive relations are easily derived because only bulk stress components are involved. The bulk constitutive relations are those of the isotropic medium to which the contribution from the shear rate associated with the weak slip surfaces is added. If the isotropic medium is a power-law fluid and the slip law is nonlinear, the bulk constitutive relations in principal coordinates x' and y' parallel and normal to the slip planes are

$$D'_{xx} = BJ_2^{[(n-1)/2]} s'_{xx},$$
$$D'_{xy} = \left\{BJ_2^{[(n-1)/2]} + B^*\left[\left(s'_{xy}\right)^2\right]^{[(n^*-1)/2]}\right\} s'_{xy}. \tag{6}$$

where B^* and n^* are constants in the nonlinear slip law. Since J_2 is an *isotropic* invariant, it is not necessary to refer it to the principal coordinates.

To illustrate the behavior of this material, consider a set of periodic, upright chevron folds, symmetric about their axial planes. Let θ be the limb-dip, initially small, but not in this case restricted to small values, and refer quantities to fixed axes x and y normal and parallel to the axial plane. Substitute

$$s'_{xy} = -s_{xx}\sin 2\theta + s_{xy}\cos 2\theta \tag{7}$$

into the slip term in Eq. (6) and assign its contributions to D_{xx} and D_{xy} using the transformation relations

$$\left(D_{xx}\right)_{\mathrm{SLIP}} = -\left(D'_{xy}\right)_{\mathrm{SLIP}}\sin 2\theta,$$
$$\left(D_{xy}\right)_{\mathrm{SLIP}} = -\left(D'_{xy}\right)_{\mathrm{SLIP}}\cos 2\theta. \tag{8}$$

Thus,

$$D_{xx} = BJ_2^{[(n-1)/2]} s_{xx} - B^* \times \left[\left(-s_{xx}\sin 2\theta + s_{xy}\cos 2\theta\right)^2\right]^{[(n^*-1)/2]} \times \left(-s_{xx}\sin 2\theta + s_{xy}\cos 2\theta\right)\sin 2\theta,$$
$$D_{xy} = BJ_2^{[(n-1)/2]} s_{xy} + B^* \times \left[\left(-s_{xx}\sin 2\theta + s_{xy}\cos 2\theta\right)^2\right]^{[(n^*-1)/2]} \times \left(-s_{xx}\sin 2\theta + s_{xy}\cos 2\theta\right)\cos 2\theta \tag{9}$$

Evolution of a symmetric chevron fold may be described by the relation (e.g. Bayly, 1964; Fletcher and Pollard, 1999)

$$\mathrm{d}(\tan\theta)/\mathrm{d}t = (\mathrm{d}\theta/\mathrm{d}t)(1 + \tan^2\theta) = 2(D_{xy} - D_{xx}\tan\theta). \tag{10}$$

Since, in the symmetric case considered here, $s_{xy} = 0$ and $s_{xx} < 0$, an explicit chevron folding solution may be obtained from Eqs. (9) and (10) for the special case $n^* = n$.

Combining these, the evolution equation becomes

$$\mathrm{d}(\tan\theta)/\mathrm{d}t = -2D_{xx}\left\{\left(B^*/B\right)\left(\sin^2 2\theta\right)^{[(n-1)/2]}\cos 2\theta \sin 2\theta\left[1+\left(B^*/B\right)\left(\sin^2 2\theta\right)^{[(n-1)/2]}\right]^{-1}\right\}. \tag{11}$$

This may be integrated numerically to give limb dip as a function of bulk shortening for a prescribed initial dip, $\theta(0)=\theta_0$. The deviatoric stress for a given rate of shortening is

$$|s_{xx}| = \frac{|D_{xx}|^{1/n}}{B + B^*(\sin^2 2\theta)^{[(n-1)/2]}} \tag{12}$$

The signs of s_{xx} and D_{xx} are both negative.

Fig. 1 shows limb-dip versus stretch parallel to the axial plane for the ratio $B^*/B=2$ and stress exponents $n=1$, 2, 3, 5, 10 and 100 for an ideal, straight limbed chevron fold with an initial limb-dip of 1°. In relation to the more commonly used $m=\eta_n/\eta_s$ in the linear case, $B^*/B=m-1$, but this relationship is not useful in the nonlinear case. For fixed B^*/B initial amplification is sluggish unless $n=1$; note that the range in stretch is extremely large. The limit behavior as n increases, which is independent of the ratio B^*/B, is obvious from the relation (11).

In the evolution equation (11) the *perturbation* itself, θ, enters explicitly, and if $\theta_0=0$, no folding occurs. That is, the linearized form of Eq. (11), to terms $\sim\theta$, is the final result of a stability analysis for this symmetric case. Accordingly, the question arises as to how the formulation and analysis of either Cobbold et al. (1971) or Latham (1985a,b), in which explicit consideration of a geometric perturbation does not enter, can apply to the case of a linear or nonlinear *fluid*.

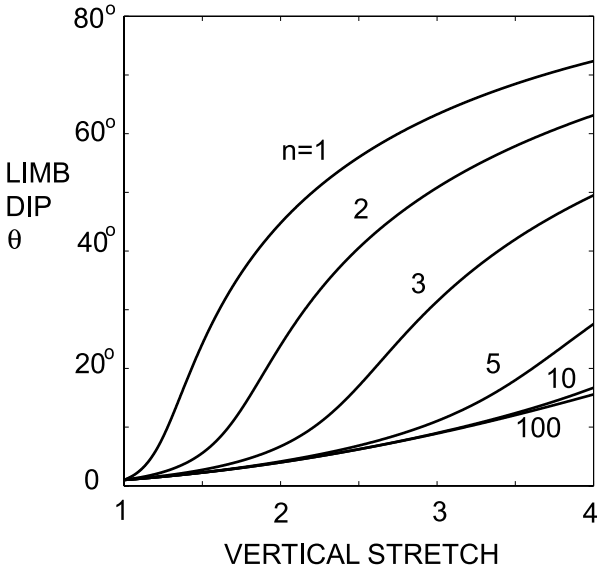

Fig. 1. Limb-dip θ (vertical axis, in degrees) of ideal chevron fold versus axial plane parallel stretch (horizontal axis) for IMSS materials with stress exponents $n=1$, 2, 3, 5, 10, and 100 and $B^*/B=2$.

2.3. Alternative constitutive relations

The IMSS relations are appropriate for rocks with slip surfaces or thin very soft layers and continuous stiff layers of uniform thickness, so that slip surfaces within a representative volume are parallel and planar. Rocks best described as made up of lenticular stiff elements separated by anastomosing weak surfaces or weak matrix do not possess this kind of regularity. With rocks such as these in mind (see Discussion), we formulate another equally simple set of constitutive relations.

The constitutive relations may be formulated by using a scalar *anisotropic* invariant (e.g. Hill, 1950):

$$Y_2' = \left(s_{xx}'\right)^2 + a^2\left(s_{xy}'\right)^2. \tag{13}$$

to replace the *isotropic* invariant, J_2. Y_2' is only invariant for discrete coordinate rotations of 90° about the z-axis. The isotropic power-law, specialized for plane flow, may be written (Calladine and Drucker, 1962)

$$D_{xx} = \partial\Pi/\partial\sigma_{xx}, \quad D_{yy} = \partial\Pi/\partial\sigma_{yy}, \quad D_{xy} = \partial\Pi/\partial\sigma_{xy}, \tag{14}$$

where

$$\Pi = [2B/(n+1)]J_2^{[(n+1)/2]}. \tag{15}$$

For the case of plane flow

$$J_2 = 1/4\left(\sigma_{xx}-\sigma_{yy}\right)^2 + (1/2)\left(\sigma_{xy}^2+\sigma_{yx}^2\right), \tag{16}$$

and in the differentiation, σ_{yx} and σ_{xy} are taken as distinct (Calladine and Drucker, 1962).

A surface $\Pi=$constant is one for which the rate of dissipation is the same at any stress point. Generalization to an anisotropic material is obtained by using the form

$$\Pi' = [2B/(n+1)]\left(Y_2'\right)^{[(n+1)/2]} \tag{17}$$

in Eq. (14), where

$$Y_2' = 1/4\left(\sigma_{xx}'-\sigma_{yy}'\right)^2 + \left(a^2/2\right)\left[\left(\sigma_{xy}'\right)^2+\left(\sigma_{yx}'\right)^2\right]. \tag{18}$$

This yields the relations

$$D_{xx}' = B\left(Y_2'\right)^{[(n-1)/2]}s_{xx}', \quad D_{xy}' = B\left(Y_2'\right)^{[(n-1)/2]}\left(a^2 s_{xx}'\right). \tag{19}$$

Comparing these relations with those for the bilaminate power-law fluid (Eq. (2)), we may anticipate moderate to large differences in behavior.

In contrast to the IMSS materials with varying n, chevron folding in this material is: (i) independent of n, and (ii)

exactly equivalent to that of a layered viscous fluid with the identification $a^2=m$. To see this, repeat the steps of the previous analysis. For example, we find

$$\frac{D_{xy}}{D_{xx}}=\frac{-\left(a^2-1\right)\sin 4\theta}{\left(a^2+1\right)-\left(a^2-1\right)\cos 4\theta}. \tag{20}$$

Thus, whatever microscopic configuration of nonlinear components might result in a fluid with constitutive relations of the form (19), it is not equivalent to a nonlinear IMSS material. This *Y_2-fluid* shows strong instability at small limb-dip as opposed to the sluggish behavior of the IMSS material.

3. Analysis of instability in the Y_2 fluid

The general form of a linearly-independent component in the perturbation in orientation of the foliation must be taken as

$$\theta(x,y)=-\Theta\sin[\lambda(x-\nu y)]. \tag{21}$$

Such components retain their forms, except for changes in Θ, λ, and ν, during finite basic-state deformation. They are linearly-independent because they do not interact. As a partial illustration of this, in a finite deformation involving basic-state foliation parallel shear, the symmetric form

$$\begin{aligned}\theta(x,y)&=-(\Theta/2)\left\{\sin\left[\lambda(x-\nu y)\right]+\sin\left[\lambda(x+\nu y)\right]\right\}\\&=-\Theta\sin(\lambda x)\cos(\lambda\nu y)\end{aligned} \tag{22}$$

'breaks up' into two component forms, the parameters of which do not remain equal. Otherwise, the evolving form would have to retain its initial symmetry, which is impossible with shear parallel to foliation.

The height of the trace of foliation above its mean height y may be written

$$\zeta(x,y)=A\cos[\lambda(x-\nu y)]. \tag{23}$$

In the present analysis, only the approximation for $\theta\ll 1$ is treated, for which

$$\theta\cong\tan\theta=\partial\zeta/\partial x, \tag{24}$$

and

$$\Theta=-\lambda A. \tag{25}$$

Consider the general basic-state flow

$$\bar{v}_x=\bar{D}_{xx}x+2\bar{D}_{xy}y,\quad \bar{v}_y=-\bar{D}_{yy}y, \tag{26}$$

where $\bar{D}_{xx}$ and $\bar{D}_{xy}$ are homogeneous rate of deformation components. These might be independent functions of time, but here they are treated as having constant ratio.

The first step in the analysis is to obtain the approximate, linearized form of the constitutive relations in x and y coordinates taking into account the local deflection in foliation, θ, and retaining only first-order terms in this quantity. The parameters B and a^2 might also vary slightly about their mean values, but we do not treat this possibility here. With contributions to the perturbed quantities from θ only, we obtain the linearized relations for the perturbing quantities, with, for example, $D_{xx}=\bar{D}_{xx}+\tilde{D}_{xx}$,

$$\begin{aligned}\tilde{D}_{xx}&\cong B\bar{Y}_2^{[(n-1)/2]}\left\{\left[\left(n\bar{s}_{xx}^2+a^2\bar{s}_{xy}^2\right)/\bar{Y}_2\right]\left[\tilde{s}_{xx}+2\left(1-a^2\right)\bar{s}_{xy}\theta\right]\right.\\&\quad\left.+\left[(n-1)a^2\bar{s}_{xx}\bar{s}_{xy}/\bar{Y}_2\right]\tilde{s}_{xy}\right\},\\\tilde{D}_{xy}&\cong B\bar{Y}_2^{[(n-1)/2]}\left\{\left[(n-1)a^2\bar{s}_{xx}\bar{s}_{xy}/\bar{Y}_2\right]\tilde{s}_{xx}\right.\\&\quad\left.+\left[\left(\bar{s}_{xx}^2+na^2\bar{s}_{xy}^2\right)/\bar{Y}_2\right]\left[\tilde{s}_{xy}+2\left(1-a^2\right)\bar{s}_{xx}\theta\right]\right\},\end{aligned} \tag{27}$$

where

$$\bar{Y}_2=\bar{s}_{xx}^2+a^2\bar{s}_{xy}^2.$$

We seek the *particular* solution of the equation of rate of deformation compatibility for the case that θ is given by Eq. (21). The compatibility equation is

$$\partial^2\tilde{D}_{xx}/\partial y^2+\partial^2\tilde{D}_{yy}/\partial x^2-2\partial^2\tilde{D}_{xy}/\partial x\partial y=0. \tag{28}$$

We write the deviatoric stress components in terms of the Airy stress function

$$\tilde{s}_{xx}=(1/2)\left(\partial^2\phi/\partial y^2-\partial^2\phi/\partial x^2\right),\quad \tilde{s}_{xy}=-\partial^2\phi/\partial x\partial y. \tag{29}$$

Entering these quantities in Eq. (27) and substituting the results in Eq. (28) gives

$$\begin{aligned}&\partial^4\phi/\partial y^4-4N\partial^4\phi/\partial y^3\partial x+2(2Ma^2-1)\partial^4\phi/\partial y^2\partial x^2\\&\quad+4N\partial^4\phi/\partial y\partial x^3+\partial^4\phi/\partial x^4\\&=4(a^2-1)\left[\left(\partial^2\theta/\partial y^2-\partial^2\theta/\partial x^2\right)\bar{s}_{xy}-2M\left(\partial^2\theta/\partial x\partial y\right)\bar{s}_{xx}\right],\end{aligned} \tag{30}$$

where

$$M=\frac{\bar{D}_{xx}^2+n\bar{D}_{xy}^2/a^2}{n\bar{D}_{xx}^2+\bar{D}_{xy}^2/a^2},$$

$$N=\frac{(n-1)\bar{D}_{xx}\bar{D}_{xy}}{n\bar{D}_{xx}^2+\bar{D}_{xy}^2/a^2}.$$

The basic-state relations between rate of deformation components and deviatoric stress components

$$\bar{D}_{xx}=B\bar{Y}_2^{[(n-1)/2]}\bar{s}_{xx},\quad \bar{D}_{xy}=B\bar{Y}_2^{[(n-1)/2]}\left(a^2\bar{s}_{xy}\right), \tag{31}$$

have been used to replace deviatoric stress components with rate of deformation components. The relation (30) is used to obtain the stress function ϕ, the deviatoric stresses obtained from it through (29) are substituted into the relations (27) which are then integrated to give the velocity components.

The rate of amplification of slope may then be found

$$\mathrm{d}(\lambda A)/\mathrm{d}t = \left(-\bar{D}_{xx} + q_{\mathrm{MECH}}\right)(\lambda A) = q(\lambda A), \tag{32}$$

where

$$q_{\mathrm{MECH}} = -4\left(a^2-1\right)\left\{\left[\left(1-v^2\right) - 2Nv\right]M^*\bar{D}_{xx} - \left[N^*\left(1-v^2\right) - 2M^*v\right]\bar{D}_{xy}\right\}\left[\left(1-v^2\right)^2 - 4Nv\left(1-v^2\right) + 4Ma^2v^2\right]^{-1},$$

and

$$M^* = \Lambda M,$$

$$N^* = \Lambda N/a^2,$$

$$M = \frac{\left(\bar{D}_{xx}^2 + n\bar{D}_{xy}^2/a^2\right)}{\left(n\bar{D}_{xx}^2 + \bar{D}_{xy}^2/a^2\right)},$$

$$N = \frac{(n-1)\bar{D}_{xx}\bar{D}_{xy}}{\left(n\bar{D}_{xx}^2 + \bar{D}_{xy}^2/a^2\right)},$$

$$\Lambda = \frac{\left(n\bar{D}_{xx}^2 + \bar{D}_{xy}^2/a^2\right)}{\bar{Y}_2}.$$

The evolution equations are completed by the relations

$$\mathrm{d}\lambda/\mathrm{d}t = -\bar{D}_{xx}\lambda, \quad \mathrm{d}v/\mathrm{d}t = 2\bar{D}_{xy} + \bar{D}_{xx}v. \tag{33}$$

These are required to account for finite deformation associated with the basic-state.

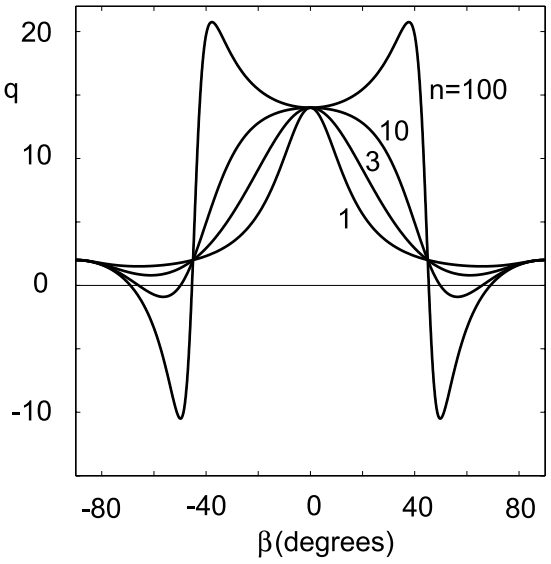

Fig. 2. Orthotropic case for shortening parallel to mean foliation: growth rate $q(\beta)$ for $a^2=4$ and $n=1$, 3, 10, and 100. See text for discussion.

4. Results

4.1. Orthotropic cases

Amplification of band-like perturbations is illustrated in Fig. 2 by plotting q versus β for a case of moderate anisotropy, $a^2=4$, and for $n=1$, 3, 10, and 100. q is evaluated for foliation parallel shortening, but the results for extension may be read off the diagram by merely switching the sign of q. The linear viscous case, $n=1$, shows the expected maximum for bands or crenulations with axial plane normal to foliation. Indeed, from Eq. (32), amplification of a component at $\beta=0$, or $v=0$, is independent of n, with $q(0;\, a^2,\, n) = -\mathrm{Sgn}(\bar{D}_{xx})[4(a^2-1)+1]$, where $\mathrm{Sgn}(X)$, the signum function of argument X, is $+1$ for $X>0$, 0 for $X=0$, and -1 for $X<0$. Perturbations of all orientations are amplified, at least by kinematic, or passive, amplification, though at large β amplification is slightly less than kinematic. For modest nonlinearity, $n=3$, the peak in q broadens, and flanking minima of negligible magnitude occur at $\beta \approx 60°$ and $-60°$. At $n=10$, the peak is very broad, and minima with values of -2 occur at $\beta \approx 55°$ and $-55°$. In extension, these minima would be peaks corresponding to weak amplification of internal boudinage. Here, it is too weakly amplified to develop. At very large nonlinearity, $n=100$, the behavior in shortening is qualitatively different, with large peaks at $\beta \approx 35°$ and $-35°$. Folding consists of conjugate sets of crenulations separated by $\approx 70°$. The effect of the basic-state shortening is to decrease the magnitude of β of a component, so that the angle between 'sets' would be expected to decrease. In extension, strong peaks for internal boudinage are present at $\beta \approx 50°$ and $-50°$. Components in the perturbation at smaller angles to the foliation normal will tend to be de-amplified. Maximum amplification in extension will accordingly tend to occur between the peaks and the positions where $q=0$, or $\beta \approx 45°$ and $-45°$. As opposed to folding, internal boudinage must 'lock-in' by some mechanism at finite amplitude to avoid subsequent de-amplification. In the orthotropic case, three types of structures might form, depending on the value of the quantity a^2/n, since a^2-1 simply scales the magnitude of q, excluding the kinematic term. These are symmetric upright crenulation, conjugate folds, and symmetric boudinage. The transition between vertical and conjugate crenulation may be identified by plotting q with the kinematic part and the factor $-(a^2-1)\mathrm{Sgn}(\bar{D}_{xx})$ excluded. This is only a function of a^2/n. The curves, not shown, broaden and then show weak conjugate maxima at about $a^2/n=0.1$, where the transition occurs.

4.2. Simulation of structure in shortening or extension alone parallel to mean foliation

Fold structures that might appear in naturally deformed rock may be simulated by amplifying an initial random perturbation. Since the analysis only applies for $\theta \ll 1$, full

comparison with natural structures that have foliation at angles of 20°–60° to enveloping surfaces, requires additional analysis not carried out here.

In these simulations, initial components have inclinations from −88° to 88° at intervals of 1°. Each component is assigned a random phase shift and a random wavelength, over a limited range of the latter. Beginning with such a 'random' set of perturbations and following their evolution over a finite deformation, a realization of the structure formed for some pair of values a^2 and n is obtained. Since the amplitude spectrum in the finite series expansions for slope that is computed is not tapered as wavelength decreases, the smaller wavelengths dominate. Thus, the patterns tend to show a strong regularity in scale of the structures, not unlike natural structures. The results indicate the kinds of structures produced, but do not establish a basis for extracting valid statistics on spacing and persistence of individual structures. Fig. 3a shows a 'random' initial perturbation. In the simulations, a different initial perturbation is generated for each realization. Amplitude in these figures is adjusted upwards to produce a visually distinct image; the first-order analysis does not strictly provide a valid approximation for the slope magnitudes shown.

Folding after shortening of ∼15% for $n=1$, $a^2=4$ (Fig. 3b) yields the expected upright crenulations for an anisotropic viscous fluid. Folding of a highly nonlinear fluid with $n=100$, $a^2=4$, or $a^2/n=0.04$, for shortening of ∼15% (Fig. 3c) yields conjugate bands. Internal boudinage in the same fluid is obtained at ∼16% extension (Fig. 3d) at the expected orientation of 'normal kink bands.'. Structures obtained in simulations with different initial perturbations are quite variable. In particular, even though the bulk deformation is foliation-parallel extension or shortening, the structures may locally show marked asymmetry.

4.3. Combined shortening or extension and shear parallel to the mean foliation

The only geometric factor influencing instability is band orientation, $\beta=\tan^{-1}(v)$. The kinematic factor is the ratio of foliation-parallel shortening or extension, $\bar{D}_{xx}$, and foliation-parallel shear, $\bar{D}_{xy}$. In the analysis, the x-axis is fixed in the direction of mean foliation. A rotation of the foliation relative to some other set of fixed axes has no influence on folding except as it affects the histories of $\bar{D}_{xx}$ and $\bar{D}_{xy}$. Here, we only consider the case of a constant ratio $\bar{D}_{xx}/\bar{D}_{xy}$,

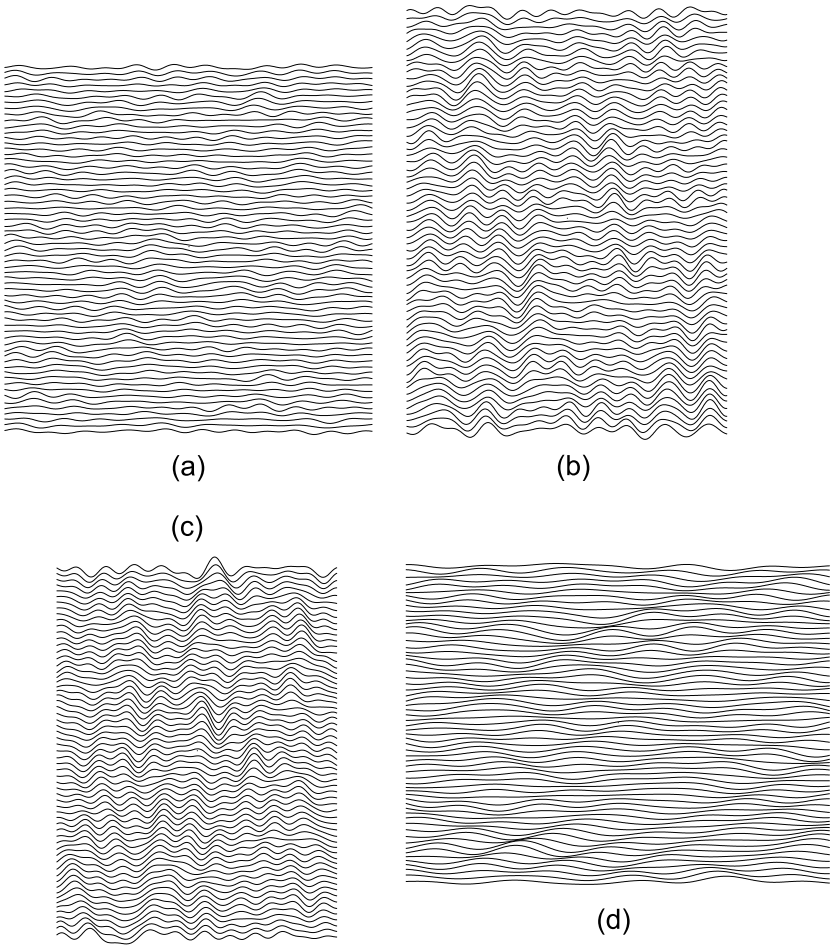

Fig. 3. Finite strain simulations in pure shear. The finite strain is indicated by the shape of the boxes, which were initially square. (a) Initial state showing random perturbations. (b)–(d) Deformed states, see text for discussion.

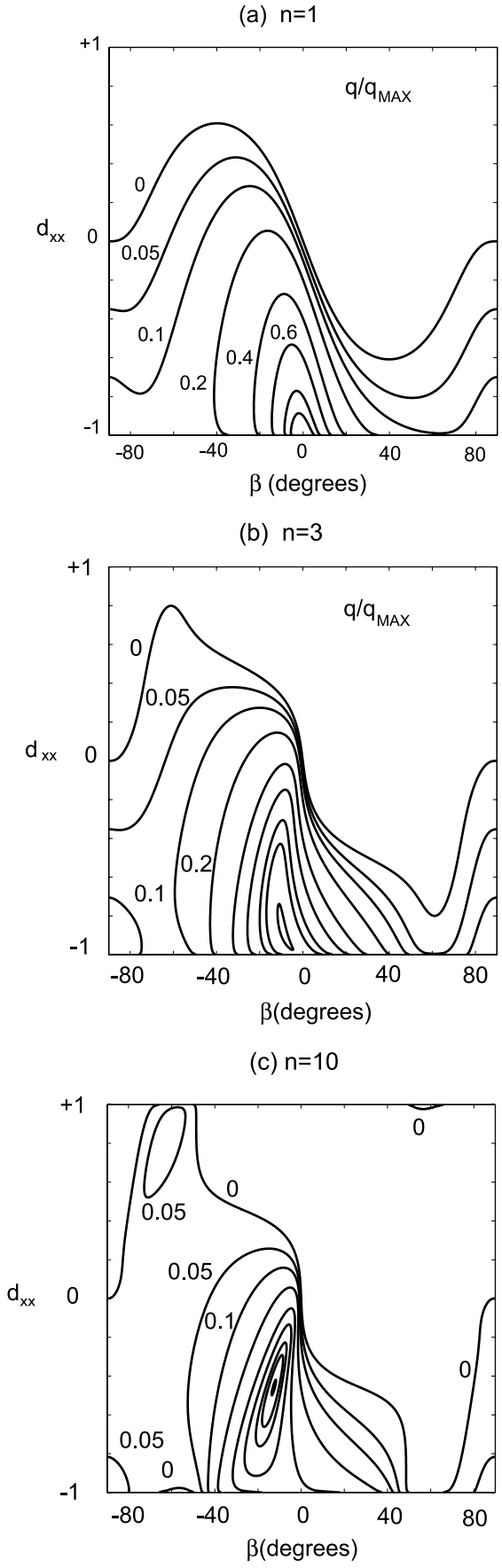

$\bar{D}_{xy} \geq 0$. Here, we use dimensionless quantities

$$d_{xx} = \bar{D}_{xx}/\bar{I}_2^{1/2}, \quad d_{xy} = \bar{D}_{xy}/\bar{I}_2^{1/2}, \quad \bar{I}_2 = \left(\bar{D}_{xx}\right)^2 + \left(\bar{D}_{xy}\right)^2. \tag{34}$$

Since

$$d_{xy} = \left(1 - d_{xx}^2\right)^2. \tag{35}$$

d_{xx} fully describes the basic-state flow. Behavior of a given material, specified by n and a^2, may then be represented in the β, d_{xx}-plane.

Consider the relative rate of amplification, q (Eq. (32)). To illustrate the conditions under which instability in an anisotropic rock mass is strong, we plot contours of $q/q_{\max}$, where $q_{\max}$ is the maximum value of q over the entire range $-90° \leq \beta \leq 90°$ and $-1 \leq d_{xx} \leq +1$. Only positive contours are plotted because the negative contours are related by a center of inversion at $d_{xx}=0$, $\beta=0$.

For a linear viscous medium, $n=1$, with moderate anisotropy, $a^2=4$ (Fig. 4a), the maximum instability, $q_{\max}=14$, is for a component with axial plane normal to the mean foliation in foliation-parallel shortening. An interesting new result is the presence of weak instability in simple shear, $d_{xx}=0$, extending into the region of combined shear plus extension. The maximum instability in simple shear has $q/q_{\max} \approx 0.25$ for a band inclined at $\beta \approx -15°$, in a 'reverse-drag' sense. Because band inclination changes continuously, and the instability is weak, cumulative amplification cannot be accurately computed by assuming q for the component is constant, but a generous upper bound is found by this approximation. For a shear $\Gamma=1$, the amplification is only ≈ 6. The asymmetry of q about $\beta=0$ means that after the band passes through an orientation normal to the mean foliation, the perturbation decays. For a fold structure to be preserved, the perturbation must reach a slope sufficient to achieve a 'locked-in' status by some mechanism.

For $n=3$ (Fig. 4b), the contour $q/q_{\max}=0.995$ is inserted to show that the maximum rate of amplification occurs with a small increment of superposed shear, and shifts to a component with $\beta \sim -10°$. In this case, the effect is quantitatively negligible. While folding of a single embedded layer of isotropic power-law fluid is substantially enhanced as the stress exponent increases, this is not so for the present anisotropic medium; the maximum value of q is only a few percent higher than that for $n=1$. At $n=10$ (Fig. 4c), maximum q has now more than doubled from that for $n=3$. The largest value occurs for $d_{xx} \sim 0.5$, corresponding to a ratio $\bar{D}_{xx}/\bar{D}_{xy} \sim -1.7$; equal rates of shear and shortening correspond to $d_{xx} = -0.707$ or $+0.707$. Weak instability occurs in foliation-parallel extension, $d_{xx}=1$.

Fig. 4. Values of $q/q_{\max}$ in β, d_{xx}-space. Contours are 0, 0.05, 0.1, 0.2, 0.4, 0.6, 0.8, 0.9, and 0.995; all are not shown in any one figure. The horizontal axis is band orientation β in degrees and the vertical axis is d_{xx}. The values of $q_{\max}$ are: (a) 14, (b) 14.1, and (c) 32.6.

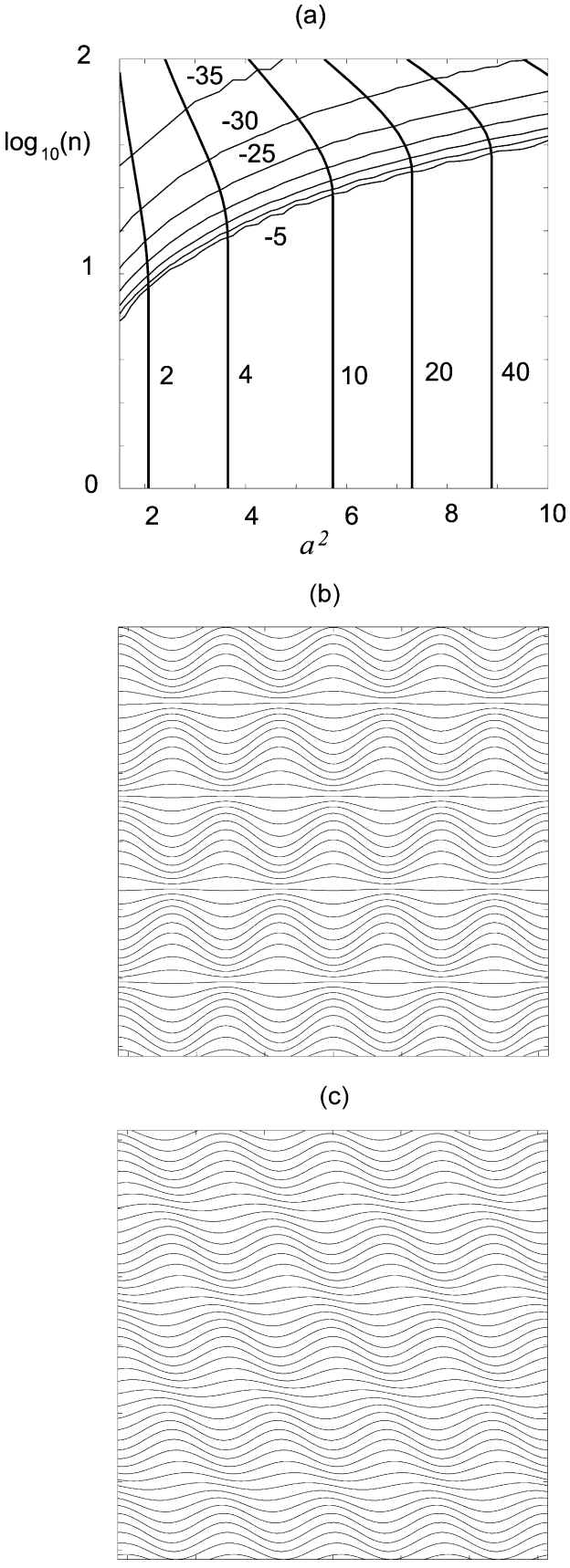

Fig. 5. (a) Contours of maximum amplification (thick lines) and band orientation β (thin lines) of perturbation with maximum amplification in $\log_{10}(n)$, a^2-space. (b) Symmetric structure of form according to Eq. (22). (c) Asymmetric structure of the same type corresponding to the amplitude of the left-dipping band equal to half that of the right-dipping bands.

Taking finite deformation into account by integrating Eqs. (19) and (20), the component that has received the maximum cumulative amplification may be identified. Fig. 5a gives the result for foliation-parallel pure shear at 10% shortening. For $n<10$, characteristic of much ductile behavior of rock, upright folds are formed. At large n maximum amplification occurs for inclined bands. In pure shear, conjugate bands at equal but opposite inclination amplify by the same amount. A structure of this type with conjugate bands at $\beta=+30°$ and $-30°$ is shown in Fig. 5b. The amplitude is exaggerated; the solution only applies when slope is small. Such a mode is termed self-confined (Biot, 1965b). The nodal planes, or planes of zero amplitude, are not precisely captured. This perturbation is more strongly amplified than a symmetric fold for a rheological behavior that is nearly rigid plastic. For initial conditions with amplitude of one band half that of the other, the conjugate structure is less apparent (Fig. 5c).

Because amplification is followed by de-amplification in simple shear, it is useful to consider the behavior in finite strain. For a shear strain of $\Gamma=2\bar{D}_{xy}t=0.4$, amplification is low unless n is very large (Fig. 6). Once shear carries the most amplified band past the normal to foliation, it decays. Consequently, amplification for positive values of β does not increase with larger amounts of shear. Some amplification does occur for materials with properties reasonable for ductile rock behavior: $n=1$–5, $a^2=2$–10, but amplifications of 2–4 are not likely to initiate structures. Augmentation by a small amount of shortening greatly enhances amplification. Foliation inclined slightly in the direction of shear within a shear zone, would be subjected to such shortening, and folds would be produced in any case. The fact that simple shear results in some amplification, coupled with the existence of other amplification mechanisms (Lister and Williams, 1979; Cobbold and Quinquis, 1980; Alsop and Holdsworth, 2002), such as perturbations in shear zone thickness, increase the likelihood of producing fold structures in shear zones and similar high-shear settings.

Fig. 7a shows maximum amplification and band inclination at a nominal strain $\exp(\bar{I}_2t)=1.1$ as a function of n and a^2 for $\bar{D}_{xx}=-\bar{D}_{xy}$, $\bar{D}_{xy}>0$. Amplification is substantial for large n and a^2, but the maximum amplification required for structures to persist at finite deformation depends on the magnitude of the initial perturbations. It seems reasonable to suppose that the transition between selective amplification and finite-amplitude evolution occurs at maximum slopes of 10°–15°. If the initial magnitude of the perturbation is 0.5°–1°, the required amplification is 20–40. For this small strain, a viscous medium, $n=1$, must possess very high anisotropy, $a^2>10$. Only moderate anisotropy, $a^2>4$, is required for a strongly anisotropic material, $n=10$. Axial planes of components

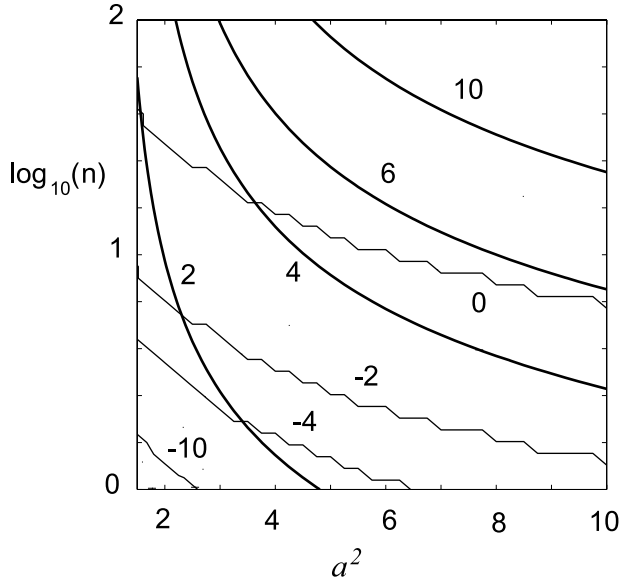

Fig. 6. Amplification in simple shear for a shear strain $\Gamma=0.4$. Thick contours are maximum amplification and thin contours are orientation of the most-amplified component.

with strong amplification are inclined at a small angle to the foliation normal in the reverse-drag sense.

Fig. 7b gives the results for foliation-parallel extension $\bar{D}_{xx}<0$, $\bar{D}_{xy}=0$ at $\exp(I_2 t)=1.22$; a larger range in n is covered. Large values of n represent a rigid-plastic solid at yield or, approximately, quasi-brittle behavior. Recall that large values of n may arise in an approximate analysis of strain softening materials (Neurath and Smith, 1982). Here, values $n>50$–100 are required to reach a maximum amplification >20. If the material were truly plastic or brittle, instability would set in after minimal strain. The relatively weak dependence on the strength of anisotropy, a^2, above a value of 3 or 4 is of interest. The structure represented here is internal boudinage or internal necking (Cobbold et al., 1971; Platt and Vissers, 1980). In pure extension, two band orientations yield maximum amplification; only the negative value is given here.

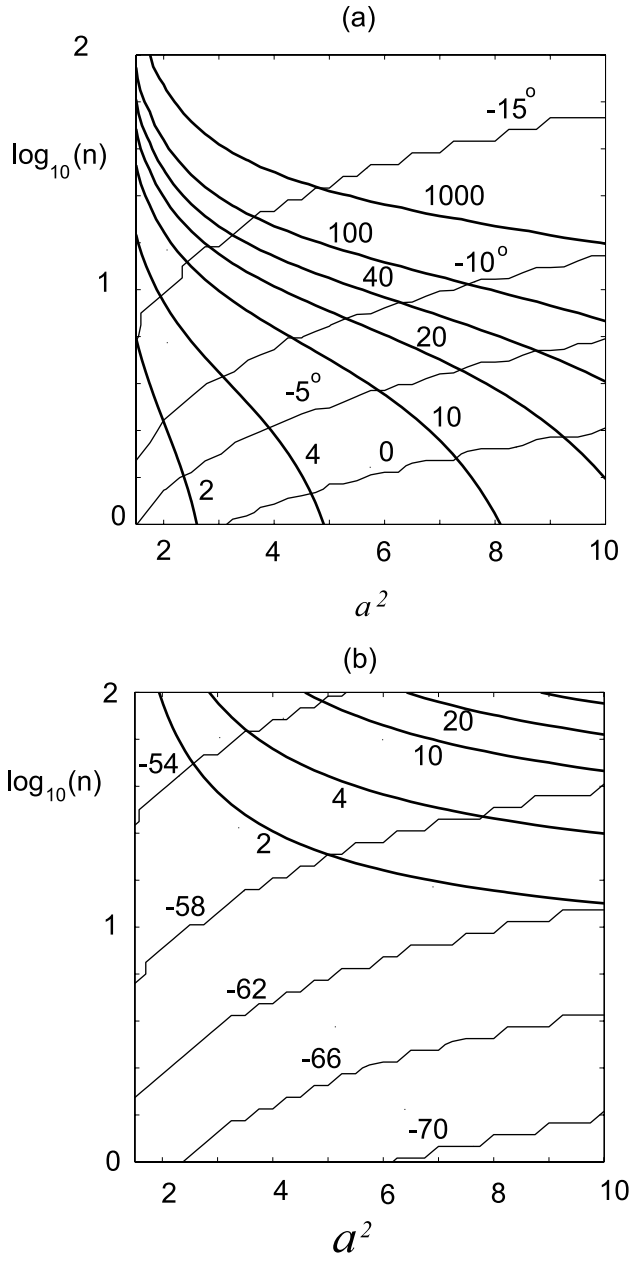

Fig. 7. As in Fig. 6, but for (a) $D_{xx}=-D_{xy}<0$; and (b) $D_{xx}=1$, $D_{xy}=0$.

5. Discussion

5.1. What kinds of composite rocks are approximated by the Y_2-fluid?

Application of the Y_2-fluid constitutive relations for plane flow of an anisotropic power-law fluid (Eq. (11)) is supported by their simplicity. Recall that the isotropic relations themselves are not constructed ab initio from the properties of the elementary components of a rock. For example, they might typically be applied to a rock consisting of one or more mineral components, single crystals of which are anisotropic in their rheological behavior. The isotropic relations are adequate as long as the lattice preferred orientations of the minerals are weak and strongly inequant aggregates of the minerals are not present. Thus, ab initio construction of constitutive relations, which may easily be done for layered materials, is not always thought of as a necessary test of applicability. Nonetheless, it would be useful to show that the Y_2-fluid approximation arises naturally for some configurations of constituents likely to represent natural composite rocks. In this case, we would be able to estimate the parameter a^2 in the same way that η_n and η_s may be estimated for a laminated viscous fluid.

The generalization was first suggested by consideration of the yield condition and flow law for an incompressible anisotropic plastic solid (Hill, 1950). For an isotropic von

Mises plastic solid, specialized for plane flow, the yield condition is:

$$J_2 = s_{xx}^2 + s_{xy}^2 = K^2, \tag{36}$$

and the flow law is:

$$D_{xx} = -D_{yy} = hs_{xx}, \quad D_{xy} = hs_{xy}, \tag{37}$$

where $h=h(x,y)$ is not a material property but a function determined from the equation of compatibility and the velocity boundary conditions.

Now suppose, as in the earlier discussion of the IMSS fluid, that the material is cut by a set of weak slip surfaces that yield at a lower resolved shear stress

$$\left(s'_{xy}\right)^2 = (K/a)^2, \tag{38}$$

where the prime denotes principal axes. The yield condition in s'_{xx}, s'_{xy}-space (Fig. 8a), consists of the segments of the circle,

$$\left(s'_{xx}\right)^2 + \left(s'_{xy}\right)^2 = K^2, \tag{39}$$

and of the two straight lines,

$$s'_{xy} = \pm K/a, \tag{40}$$

that are jointly interior to each other. The flow law corresponds to the normality of the *vector* $\left(D'_{xx}, D'_{xy}\right)$ to the yield locus. On the circular arcs, a flow law of the form (37) applies. On the straight line segments the only deformation allowed is bulk shear associated with slip on the surfaces, or

$$D'_{xx} = 0, \quad D'_{xy} = h_s s'_{xy}, \tag{41}$$

where h_s is a function of position. At the four vertices, the rate of deformation vector is not uniquely determined, but lies between its limiting orientations on the segments.

Since the state of stress is uniquely determined at the vertices, we may write for the vertex where $s'_{xx} < 0$, $s'_{xy} > 0$, for example,

$$D'_{xx} = -hK\left(1 - 1/a^2\right)^{1/2}, \quad D'_{xy} = \left(h + h_s\right)K/a. \tag{42}$$

It would be possible, for example, to solve for the evolution of seeded low-amplitude chevron folds in such a material, as in the earlier sections.

An approximation to this material is to replace the segmented yield condition, with its vertices, with the smooth inscribed ellipse

$$Y'_2 = \left(s'_{xx}\right)^2 + a^2\left(s'_{xy}\right)^2. \tag{43}$$

The flow law based on normality is then

$$D'_{xx} = hs'_{xx}, \quad D'_{xy} = h\left(a^2 s'_{xx}\right). \tag{44}$$

Many other convex surfaces might be chosen, including those more closely fitting the segmented yield surface.

Now consider what the yield condition would be if the isotropic medium were cut by two equivalent sets of weak

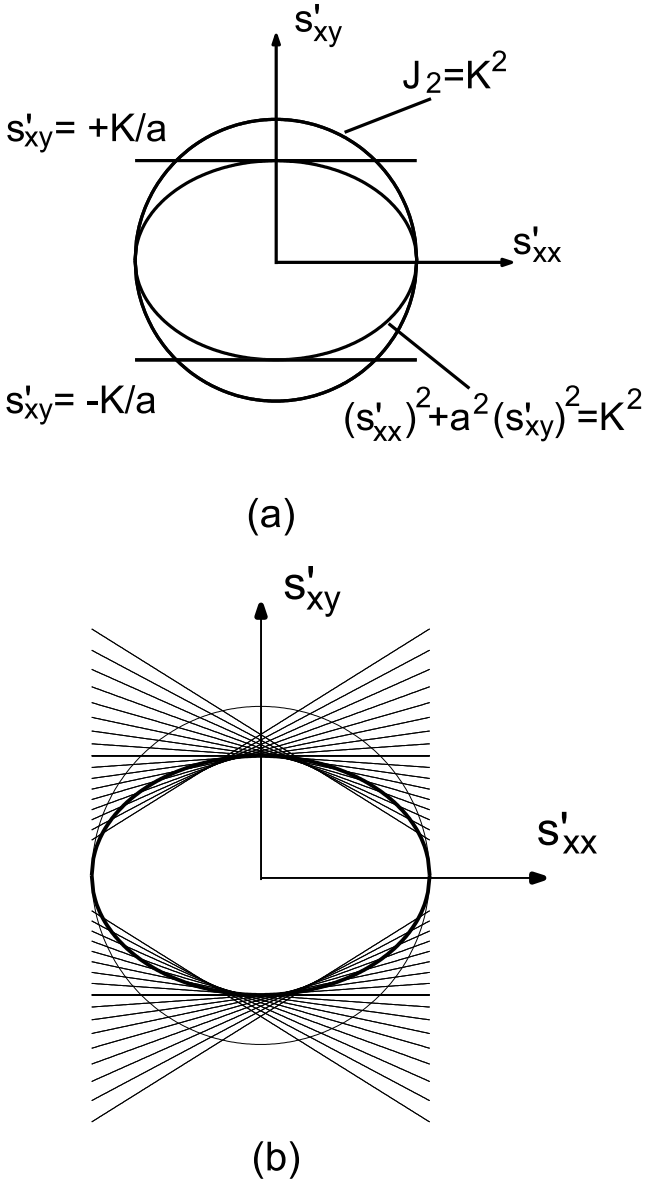

Fig. 8. Yield conditions for anisotropic plastic solids. (a) Segmented and elliptical yield surfaces for a single set of weak slip surfaces with yield stress K/a, $a=2$. (b) Elliptical yield surface for $a^2=2$ compared with that of a material with multiple sets of weak slip surfaces.

surfaces makings angles of $\pm\delta$ to the x'-axis. The conditions for slip on these sets are

$$-s'_{xx}\sin 2\delta + s'_{xy}\cos 2\delta = \pm K/a, \quad + s'_{xx}\sin 2\delta + s'_{xy}\cos 2\delta = \pm K/a. \tag{45}$$

These four straight lines define an interior diamond-shaped region. The boundary of the region jointly interior to this and to the circle of radius K is the yield locus. The locus for a single pair of slip surface sets can be 'read off' the more complex yield surface in Fig. 8b, for $a^2=2$, by selecting four lines with the same slope magnitude out of the fans of lines present. For example, the locus for sets of

surfaces at $\delta = \pm 16°$ is given by selecting the four lines with steepest slope. This locus has six vertices, two on the s'_{xy}-axis, and four where the straight lines cut the circle of radius K. Deformation associated with the former consists of dual slip on both sets of surfaces, whereas slip on the latter occurs on one set of surfaces and deformation includes that of the isotropic material. Since the slip surfaces must be viewed as material surfaces rather than the slip systems of a crystal, dual slip cannot take place without disruption of the idealized structure posited, a difficulty ignored here. The yield condition may be smoothed by supposing many additional sets of surfaces are present, filling the range between the two limiting sets. In Fig. 8b, loci for surfaces at angles $-16° < \delta < +16°$ at intervals of 2° are plotted. The yield condition is then the boundary of the interior region in Fig. 8b. In either case, the elliptical yield condition approximates the six- or four-vertex yield conditions.

Thus, the suggestion advanced is that the smooth elliptical condition, $Y_2 = K^2$, and the associated flow law, applies to composite rocks in which a marked imperfection in the regularity of a stiff-soft lamination or a single set of parallel planar slip surfaces exists. In the most easily visualized class of such materials, stiff elements are lenticular in form and are bounded by an anastomosing or web-like set of weak surfaces or of a corresponding continuous matrix of soft material. This case corresponds formally with the limit $n \to \infty$ of the anisotropic Y_2-fluid. It may be shown that the plane flow relations for any anisotropic composite made up of linear viscous components may be described by the two principal viscosities η_n and η_s. The Y_2-fluid for $n = 1$ is of this form, with $a^2 = \eta_n/\eta_s$. We accordingly hypothesize that the Y_2-fluid is an appropriate approximation for anisotropic power-law fluids of arbitrary n and with comparable internal constitution. Computations for arbitrary n that might support this hypothesis are more complex than those for the plastic limit, and have not been done. Constitutive relations in plane flow of monomineralic or polymineralic rocks with lattice preferred orientation might also be approximated by the Y_2-fluid.

5.2. Extension to three dimensions

Since the linearly independent components on the geometric perturbation are band-like, it must be possible to extend the analysis to three dimensions. A band with arbitrary dip and *strike*, relative to the mean foliation, would have associated with it a component in the perturbing flow. Such a component would consist of a plane flow, relative to a plane cutting the band and containing its normal, and an antiplane, flow in which the velocity is normal to the plane of section and dependent on the two coordinates of position within the section. Only the plane flow affects the evolution of the component in the geometric perturbation. In the nonlinear case, the plane and antiplane flows would couple. The analysis is substantially more complicated than the present one, but no real difficulty is anticipated. Such an analysis could be applied to the initiation of three-dimensional fold forms in shear zones (Alsop and Holdsworth, 2002). Such a form may be constructed as the sum of two or more band-like components. For example, Fig. 9 shows a map view of structure contours for the sum of two bands, one striking 'N–S' and the other striking 'N45°W', with relative amplitudes of 1 and 0.5. Amplification, followed by large shear strain might then produce sheath folds.

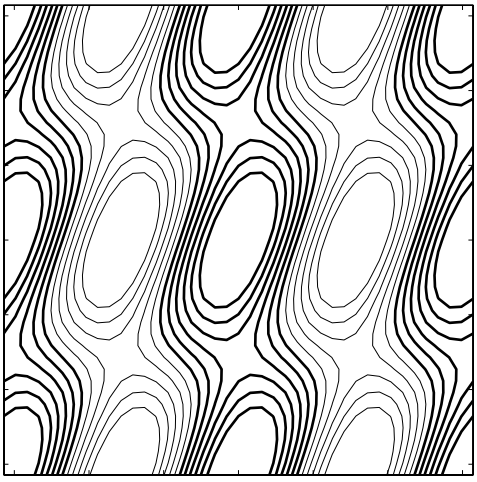

Fig. 9. Map view of foliation contours for the sum of two band-like components in the geometric perturbation in foliation.

6. Conclusions

(1) A set of constitutive relations has been formulated for an anisotropic nonlinear power-law fluid in plane flow. These reduce to the isotropic form when the anisotropy parameter $a^2 = 1$. The material does not approximate an isotropic power-law fluid cut by a single set of planar, parallel weak slip surfaces, but approximates a material in which such surfaces are irregular or anastomosing.

(2) Growth of ideal straight-limbed symmetric chevron folds in this material in shortening parallel to their axial planes at a prescribed bulk rate of shortening does not depend upon the stress exponent, n. This is also true for a bilaminate composed of two isotropic power-law fluids, both of which have the same stress exponent, $n_1 = n_2$.

(3) Non-interacting, or linearly-independent perturbations in the inclination of foliation from the mean are band-like. Amplification in a homogeneous basic-state plane flow in which both $\bar{D}_{xx}$ and $\bar{D}_{xy}$ may be non-zero gives rise to a variety of structures for a fluid with rheological parameters n and a^2. Internal boudinage requires $n >> 1$, or quasi-plastic behavior. Such large values might be achieved by strain-softening (Neurath and Smith, 1982).

(4) A weak instability is present in simple shear alone. This is distinct from that suggested by Platt (1984).
(5) The analysis may be extended to three dimensions, since linearly independent perturbations must be band-like. Hence, the resulting perturbing flow for each consists of a plane flow of the type considered here, but with different form of the coefficients as derived from the linearization of the constitutive relations, and an anti-plane flow, which will not contribute to the amplification of the perturbation.

Acknowledgements

This work was supported by NSF grant OPP-9815160. Many years ago, the author was inspired by a defective copy of John Ramsay's *Folding and Faulting of Rock*, in which a figure of a deformed trilobite was superposed on a Mohr's circle, to give up paleontology and study the physics of ductily deformed rocks. Reviews by Peter Cobbold and Martin Casey and comments by the editor Peter Hudleston (all three among the distinguished former students of John Ramsay) are greatly appreciated, and led to significant improvement of the paper.

References

Alsop, G.I., Holdsworth, R.E., 2002. The geometry and kinematics of flow perturbation folds. Tectonophysics 350, 99–125.
Bayly, M.B., 1964. A theory of similar folding in viscous materials. American Journal of Science 262, 753–766.
Bayly, M.B., 1970. Viscosity and anisotropy estimates from measurements on chevron folds. Tectonophysics 9, 459–474.
Bayly, M.B., 1974. An energy calculation concerning the roundness of folds. Tectonophysics 24, 291–316.
Biot, M.A., 1961. Theory of folding of stratified viscoelastic media and its implications in tectonics and orogenesis. Geological Society of America Bulletin 72, 1595–1620.
Biot, M.A., 1964. Exact theory of buckling of a thick slab. Applied Scientific Research, Section A 12, 183–197.
Biot, M.A., 1965a. Internal instability of anisotropic viscous and viscoelastic media under initial stress. Journal of the Franklin Institute 279, 65–82.
Biot, M.A., 1965b. Mechanics of Incremental Deformations. John Wiley & Sons, New York. 504pp.
Calladine, C.R., Drucker, D.C., 1962. Nesting surfaces of constant rate of energy dissipation in creep. Journal of Applied Mathematics 29, 79–84.
Casey, M., Huggenberger, P., 1985. Numerical modelling of finite-amplitude similar folds developing under general deformation histories. Journal of Structural Geology 7, 103–114.
Cobbold, P.R., 1976. Mechanical effects of anisotropy during large finite deformations. Bulletin of the Society of Geologists, France 18, 1497–1510.
Cobbold, P.R., Quinquis, H., 1980. Development of sheath folds in shear regimes. Journal of Structural Geology 2, 119–126.
Cobbold, P.R., Cosgrove, J.W., Summers, J.M., 1971. Development of internal structures in deformed anisotropic rocks. Tectonophysics 12, 23–53.
Fletcher, R.C., 1974. Wavelength selection in the folding of a layer with power-law rheology. American Journal of Science 274, 1029–1043.
Fletcher, R.C., Pollard, D.D., 1999. Can we understand structural and tectonic processes without appeal to a complete mechanics? Journal of Structural Geology 21, 1071–1088.
Hill, R., 1950. Theory of Plasticity. Oxford University Press. 312pp.
Latham, J.-P., 1985a. The influence of nonlinear material properties and resistance to bending on the development of internal structures. Journal of Structural Geology 7, 225–236.
Latham, J.-P., 1985b. A numerical investigation and geological discussion of the relationship between folding, kinking and faulting. Journal of Structural Geology 7, 237–249.
Lister, G.S., Williams, P.F., 1979. Fabric development in shear zones: theoretical controls and observed phenomena. Journal of Structural Geology 1, 283–298.
Neurath, C., Smith, R.B., 1982. The effect of material properties on growth rates of folding and boudinage: experiments with wax models. Journal of Structural Geology 4, 215–229.
Parrish, D., 1973. A nonlinear finite element fold model. American Journal of Science 273, 318–334.
Platt, J.P., 1984. Progressive refolding in ductile shear zones. Journal of Structural Geology 5, 619–622.
Platt, J.P., Vissers, R.L.M., 1980. Extensional structures in anisotropic rocks. Journal of Structural Geology 2, 397–410.
Sherwin, J.-A., Chapple, W.M., 1968. Wavelengths of single-layer folds: a comparison between theory and observation. American Journal of Science 266, 167–179.
Smith, R.B., 1977. Formation of folds, boudinage, and mullions in non-Newtonian materials. Geological Society of America Bulletin 88, 312–320.
Smith, R.B., 1979. The folding of a strongly non-Newtonian layer. American Journal of Science 279, 272–287.